Analytical Methods

PAPER

View Article Online
View Journal | View Issue

Cite this: *Anal. Methods*, 2015, **7**, 7511

HPLC-LTQ-orbitrap MS^n profiling method to comprehensively characterize multiple chemical constituents in xiao-er-qing-jie granules†

Yun Li,[a] Ying Liu,[b] Rongrong Liu,[a] Siyi Liu,[a] Xiuping Zhang,[a] Zijian Wang,[ab] Jiayu Zhang*[b] and Jianqiu Lu*[b]

Received 13th February 2015
Accepted 2nd July 2015

DOI: 10.1039/c5ay00420a

www.rsc.org/methods

In the present study, a method based on high performance liquid chromatography coupled with linear ion trap-orbitrap mass spectrometry (HPLC-LTQ-orbitrap) was developed for a comprehensive study of the multiple chemical constituents in xiao-er-qing-jie (XEQJ) granules, which are regularly used as a traditional Chinese medicine (TCM) for the treatment of children with high fever, sore throat, and lusterless complexion. Seven major categories of constituents preliminarily isolated from the component herbs were rapidly characterized using HPLC-LTQ-orbitrap. The fragmentation patterns of these compounds with different skeletons were clearly elaborated in the electrospray ionization (ESI) collision induced dissociation (CID)-MS/MS experiments. Based on the accurate mass measurement (<5 ppm), MS/MS fragmentation patterns, diagnostic product ions, and different chromatographic behaviors, 91 compounds were unambiguously identified or tentatively characterized, including 33 phenylethanoid glycosides, 13 phenolic acids, 11 flavonoids, 10 alkaloids, 9 lignans, 9 iridoid glycosides, and 6 saponins. Among them, 2 compounds were potential new ones from Forsythiae Fructus and 24 were unambiguously confirmed by comparing with their respective reference standards. The results demonstrated that our established method was useful and efficient to screen and identify targeted constituents from TCM extracts and other organic matter mixtures whose constituent compounds can also be classified into families on the basis of common carbon skeletons.

1. Introduction

Xiao-er-qing-jie (XEQJ) granules, which are officially listed in the Drug Standard of the Ministry of Health of the People's Republic of China, is a regularly used traditional Chinese medicine (TCM) for the treatment of children with high fever, sore throat, and lusterless complexion.[1,2] The recipe of XEQJ is composed of eight herbal medicines, *viz.*, Flos Lonicerae Japonicae (FLJ) (750 g), Forsythiae Fructus (FF) (750 g), Cortex Lycii (CL) (750 g), Indigo Naturalis (IN) (250 g), Cynanchi Atrati Radix et Rhizoma (CARR) (750 g), Radix Rehmanniae Preparata (RRP) (750 g), Pogostemonis Herba (PH) (750 g), and gypsum fibrosum (1250 g).[3]

Although the chemical constituents in the component herbs of XEQJ have been intensively studied,[4–7] little is known about the chemical composition of XEQJ, and few reports are available on its quality control. For example, Huang *et al.* determined the contents of chlorogenic acid and phillyrin in XEQJ.[8] These two chemical compositions were from only two herbs, and could not comprehensively control the quality of XEQJ. Therefore, the development of a profiling and reliable method to screen and characterize the multiple chemical constituents in XEQJ would be an important step towards a further understanding of its pharmacological effects and ultimately quality control.

With the rapid development of high performance liquid chromatography/electrospray ionization tandem mass spectrometry (HPLC/ESI-MS^n), it has played an increasingly important role in screening and identification of natural products in plant extracts in recent years.[9–12] In particular HPLC coupled with high-resolution MS (HPLC/HRMS), which can give the exact mass of analytes, has become an extremely powerful tool for characterization of phytochemical compounds of different structure types from complex matrices with its high resolution and excellent sensitivity, including flavonoids, saponins, phenolic acids, and alkaloids.[13–16] For example, the hybrid linear ion trap orbitrap mass spectrometer (LTQ-orbitrap) combined high trapping capacity and MS^n scanning function of the linear ion trap along with accurate mass measurements within 5 ppm and a resolving power of up to 100 000 over a wider dynamic range than many other mass spectrometers.[17] In

[a]*School of Chinese Pharmacy, Beijing University of Chinese Medicine, Beijing 100102, China*

[b]*Center of Scientific Experiment, Beijing University of Chinese Medicine, Beijing 100029, China. E-mail: zhangjiayu0615@163.com; lujq@vip.sina.com; Tel: +86 01064287540/01064286203*

† Electronic supplementary information (ESI) available. See DOI: 10.1039/c5ay00420a

particular, orbitrap facilitated fast data-dependent acquisition of accurate MS^n spectra on an LC timescale; these advantages could be used for increasing the throughput and identification efficiency of compounds in TCMs. Here, we first systematically report the structural characterization of the various chemical constituents of XEQJ by using HPLC-LTQ-orbitrap MS. First, the collision induced dissociation (CID)-MS/MS fragmentation pathways of some constituents ever isolated from XEQJ are proposed and then the diagnostic product ions corresponding to a certain substructure or substituent group are deduced, which could be applied to the structural characterization of serial compounds that have not been reported yet. By comparing the fragmentation patterns, retention time, and MS^n data with those of the reference standards and the literature combining accurate mass measurement, a total of 91 compounds from XEQJ were unambiguously identified or tentatively characterized, which was valuable for the quality control of XEQJ.

2. Experimental

2.1. Materials and chemicals

Eight reference standards, including rutin, luteoloside, isoquercitrin, lonicerin, calceolarioside B, isoacteoside, apigetrin, and indirubin, were obtained from the National Institutes for Food and Drug Control (Beijing, China). Sixteen reference standards of neochlorogenic acid (3-CQA), cryptochlorogenic acid (4-CQA), chlorogenic acid (5-CQA), sweroside, secoxyloganin, forsythoside A, forsythoside B, acteoside, kaempferol 3-*O*-rutinoside, isochlorogenic acid B (3,4-DiCQA), isochlorogenic acid A (3,5-DiCQA), isochlorogenic acid C (4,5-DiCQA), tricin-7-*O*-glucoside, diosmetin-7-*O*-glucoside, phillyrin, and macranthoidin A were purchased from Chengdu Biopurify Phytochemicals CO., Ltd (Sichuan, China). All these reference compounds showed purities no less than 98% by HPLC-DAD analysis. FLJ, FF, CL, IN, CARR, RRP, PH, and XEQJ were purchased from Beijing Tongrentang Medicine Corporation Ltd (Beijing, China). The material of each single herb was authenticated by Dr Jia-Yu Zhang, Center of Scientific Experiment, Beijing University of Chinese Medicine. The voucher specimen was deposited at the Center of Scientific Experiment, Beijing University of Chinese Medicine, China.

HPLC grade acetonitrile, methanol, and formic acid used were purchased from Fisher Scientific (Fisher, Fair Lawn, NJ, USA). De-ionized water used throughout the experiment was purified by a Milli-Q system (Millipore, Bedford, MA, USA).

2.2. Sample and standards preparation

For the LC-MS analysis, XEQJ and crude herbal medicines were powdered in a mortal and mill. Approximately 2.0 g pulverized powders were accurately weighed and ultrasonicated with 25 mL of 70% (v/v) methanol for 30 min, and then cooled at room temperature. The supernatant solution was filtered and evaporated on a water bath at 60 °C. The obtained residue was dissolved in 2 mL of 70% methanol. A stock solution of the reference standards was prepared in 70% methanol, which could be diluted to prepare the working solution. Prior to injection, the samples were filtered through 0.22 μm membranes. An aliquot of 10 μL of the filtrate was successively injected into the LC-HRMS instrument for analysis.

2.3. HPLC conditions

HPLC analysis was performed on an Agilent series 1100 HPLC system (Agilent Technologies, Waldbronn, Germany) equipped with a quaternary pump, an on-line degasser, a diode-array detector (DAD), an autosampler, and a column compartment. Samples were separated on a Phenomenex Luna C_{18} column (250 × 4.6 mm i.d., 5 μm) at room temperature. The mobile phase consisted of 0.1% (v/v) formic acid (A) and acetonitrile (B). A gradient program was adopted as follows: 0–26 min, 2–12% B; 26–77 min, 12–26% B; 77–80 min, 26–75% B; 80–88 min, 75–90% B; 88–94 min, 90% B. A 10 min post run time was set to sufficiently equilibrate the column. The flow rate was set at 1.0 mL min^{-1}. The DAD detector scanned from 190 to 400 nm, and the samples were detected at 254 nm.

2.4. Mass spectrometric conditions

A hybrid LTQ-orbitrap XL mass spectrometer (Thermo Scientific, Bremen, Germany) was connected to the Accela HPLC system equipped with a binary pump and an autosampler (Thermo Scientific, Bremen, Germany) *via* an ESI interface in a post-column splitting ratio of 1 : 4. For MS detection, high purity nitrogen (N_2) was used as the sheath gas and auxiliary gas, and ultra-high pure helium (He) as the collision gas. The optimized ESI parameters in the negative ion mode were as follows: capillary temperature, 350 °C; sheath gas flow, 30 arb.; auxiliary gas flow, 10 arb.; source voltage, 4.0 kV; capillary voltage, −35 V; tube lens voltage, −110 V. The analysis was performed in both negative and positive ion mode with a mass range of m/z 100–1500. In the positive ion mode, the capillary voltage was 25 V; tube lens voltage was 110 V; other parameters were same as those of negative ion mode. MS full scan was detected by high-resolution (FT) and MS/MS analysis by an ion trap dynode. Accurate mass analyses were performed according to the manufacturer's guidelines using a standard solution mixture of caffeine, sodium dodecyl sulfate, sodium taurocholate, the tetrapeptide MRFA acetate salt, and Ultramark (Sigma-Aldrich, St Louis, MO, USA). The resolution of the orbitrap mass analyzer was set at 30 000. Data-dependent MS^n scanning was used so that the two most abundant ions in each scan were selected and subjected to tandem mass spectrometry (MS^n, $n = 3$). The isolation width was 2 amu, and the normalized collision energy (CE) was 35% for all compounds. CID was conducted in LTQ with an activation q of 0.25 and activation time of 30 ms. MS scan functions and HPLC solvent gradients were controlled by the Xcalibur data system (Thermo Scientific), and all the data were collected and processed by using Xcalibur 2.1 software (Thermo Scientific).

3. Results and discussion

3.1. Optimization of analytical conditions

In order to reveal as many chemical constituents of XEQJ as possible and achieve adequate structural information of the chemical compounds with different structure types, both negative and positive modes were examined in this experiment. Generally, phenylethanoid glycosides, phenolic acids, flavonoids, lignans, and iridoid glycosides could be ionized and fragmented in the negative ion mode, while alkaloids and saponins especially C_{21} steroidal saponins preferred the positive ion mode.

3.2. HPLC/ESI-MS^n analysis of XEQJ

Fig. 1 shows the total ion chromatograms (TICs) of XEQJ and reference standards. Certain compounds in complex XEQJ matrices could be rapidly screened by using extracted ion chromatograms (EICs) with a determined narrow mass window, and then be unequivocally identified by comparison of the fragmentation patterns, retention time, chromatographic behavior, and MS^n data with those of reference standards. The diagnostic ions representing a certain substructure or substituent group were then deduced, and the fragmentation mechanisms were also proposed. Diagnostic ions and fragmentation mechanisms from reference compounds were of great importance for screening and identifying unknown compounds. For those unknown constituents, we first determined the molecular formula based on the accurate mass obtained from HRMS, and then the diagnostic ions deduced from reference standards were used to rapidly locate the candidates containing such a substructure or substituent group. Combining constituents ever isolated or reported in the literature, the most possible structure could then be determined from these candidates. Based on the described methods above, a total of 91 compounds (Tables 1, 2 and Fig. 2) were unambiguously identified or tentatively characterized from XEQJ, 24 of which were confirmed by their reference standards. Moreover, 2 of them were potential new compounds from FF. These compounds included 33 phenylethanoid glycosides, 13 phenolic acids, 11 flavonoids, 10 alkaloids, 9 lignans, 9 iridoid glycosides, and 6 saponins. The component herb from which each compound was derived was confirmed by individually analyzing seven herbs of XEQJ except gypsum fibrosum using the same HPLC/ESI/-LTQ-orbitrap MS method.

3.2.1 Structural characterization and identification of phenylethanoid glycosides. A total of 33 phenylethanoid glycosides were screened, among which 25 were from FF, 6 from PH, and 5 from RRP. Five phenylethanoid glycosides were unambiguously identified as forsythoside B (**Pg17**), forsythoside A (**Pg21**), acteoside (**Pg22**), calceolarioside B (**Pg26**), and isoacteoside (**Pg28**) by comparison with their respective reference compounds. Depending on whether the hydrogen atom in the β position was substituted, these compounds could be classified into two different types.[18]

Type I (the β position was not substituted). The ESI-MS spectrum of forsythoside B (**Pg17**) produced an $[M - H]^-$ ion at *m/z* 755.2387 ($C_{34}H_{43}O_{19}$). Its fragmentation was triggered by the initial loss of the caffeoyl unit to yield a prominent ion at *m/z* 593, and the losses of apiose and rhamnose or both were observed with the formation of ions at *m/z* 461 $[593 - 132]^-$, 447 $[593 - 146]^-$, and 315 $[593 - 132 - 146]^-$. Other minor ions at *m/z* 443, 429, and 297, corresponding to the successive loss of water from ions at *m/z* 461, 447, and 315, were also respectively detected. And another minor ion at *m/z* 179 corresponding to $[\text{caffeic acid} - H]^-$ was also observed. The proposed fragmentation pathway of forsythoside B is shown in Fig. 3. The ESI-MS/MS spectra of forsythoside A (**Pg21**) were similar to those of **Pg17**. Its $[M - H]^-$ ion yielded a lot of fragment ions at *m/z* 477, 461, 315, and 135, owing to the neutral loss of rhamnose and successive losses of the caffeoyl residue, rhamnose, hexose, and water from the $[M - H]^-$ ion at *m/z* 623.1957 ($C_{29}H_{36}O_{15}$). Acteoside (**Pg22**) and isoacteoside (**Pg28**), which were isomers of **Pg21**, had the same fragment ions as **Pg21**. Calceolarioside B (**Pg26**) gave a quasi-molecular ion at *m/z* 477.1397 ($C_{23}H_{26}O_{11}$), and two abundant fragment ions at *m/z* 161 and 315 corresponding to $[glc - H - H_2O]^-$ and $[M - H - \text{caffeoyl}]^-$. The above fragmentation behavior was in accordance with the characteristic fragmentation patterns of phenylethanoid glycosides previously reported,[19–21] and valuable in screening and deducing uncertain compounds belonging to the same class.

Pg18 yielded the identical $[M - H]^-$ ion at *m/z* 755.2389 ($C_{34}H_{43}O_{19}$) to **Pg17**, and fragmentation in the same way; it was thus assigned as an isomer of forsythoside B.

Pg13 and **Pg19** had identical molecular ions and fragmentation ions to **Pg21**, thus they were plausibly identified as isomers of forsythoside A. Considering compounds isolated from FF, forsythoside H and I were the most possible candidates. Herein, a parameter *C* log *P* was adopted to determine the elution order. *C* log *P* is the calculated value of log *P* (*n*-octanol/water partition coefficient), which is predicated by the software ChemBioDraw Version 11.0 (Cambridge-Soft, Cambridge, MA, USA) based on theoretical calculations. Generally, the compound with a larger *C* log *P* value would yield a larger retention time on reverse-phase HPLC.[22] Thus, **Pg13** and **Pg19** were tentatively characterized as forsythoside H (*C* log *P*: −0.9526) and I (*C* log *P*: −0.8902), respectively.[23]

Pg8 generated an $[M - H]^-$ ion at *m/z* 785.2494 ($C_{35}H_{45}O_{20}$), 162 Da more than **Pg21**. MS/MS of the $[M - H]^-$ ion yielded a product ion at *m/z* 623 and similar diagnostic ions to **Pg21** (Table 1); in addition, it was from RRP. Thus, this peak was characterized as that of echinacoside, a known compound isolated from RRP.[24] **Pg10** showed an $[M - H]^-$ ion at *m/z* 639.1920 ($C_{29}H_{35}O_{16}$), 16 Da higher than the base peak of **Pg21** at *m/z* 477 $[461 + 16]^-$ in the MS^2 spectrum and yielded very similar MS^3 data to **Pg21** (Table 1), indicating that rhamnose was substituted by hexose; similarly, **Pg3** had the same relationship with **Pg8**. Thus, **Pg10** and **Pg3** were potential new compounds from FF.

The spectra of **Pg11**, **Pg14**, and **Pg16** were extremely similar to that of **Pg21**, except that loss of a pentose rather than that of a rhamnose was observed. These peaks were thus identified as calceolarioside C or other unknown isomers.[18] Similarly, **Pg23** was identified as forsythoside G, a known compound isolated from FF.[18]

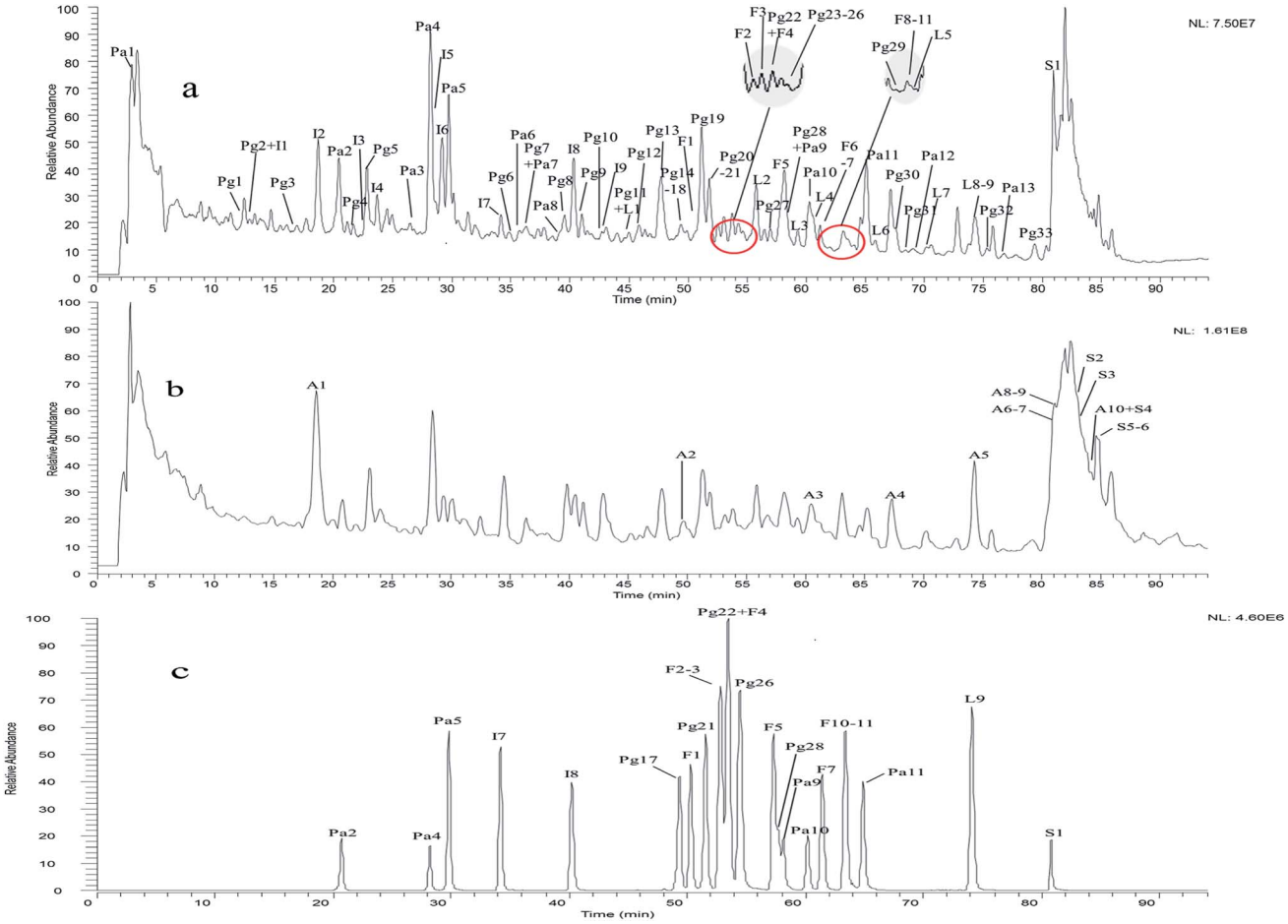

Fig. 1 ESI-MS total ion chromatograms of XEQJ and reference standards: (a) XEQJ scanned in negative ion mode, (b) XEQJ scanned in positive ion mode and (c) reference standards scanned in negative ion mode.

Pg12 showed a molecular ion at *m/z* 799.2648 ($C_{36}H_{47}O_{20}$). Its MS^3 spectrum was identical to the MS^2 spectrum of **Pg21** and it generated a base peak at *m/z* 623 formed by the loss of 176 Da from *m/z* 799. It was revealed that a methylated caffeoyl unit (176 Da) was present. **Pg24** exhibited an $[M - H]^-$ ion at *m/z* 813.2802 ($C_{37}H_{49}O_{20}$), corresponding to a fragmentation ion at *m/z* 329, which was 14 Da higher than *m/z* 315 of **Pg12**, indicating that a methoxyl group might be present in the phenylethyl moiety. Thus, **Pg12** and **Pg24** were tentatively characterized as jionoside A and jionoside B, two known compounds isolated from RRP.[25]

Both **Pg29** and **Pg31** exhibited $[M - H]^-$ ions at *m/z* 637, 14 Da higher than **Pg21**, but they had the same fragmentation pathway as **Pg21**, indicating that the caffeoyl unit (162 Da) in **Pg21** was replaced by a methylated caffeoyl unit (176 Da). Thus, leucosceptoside A from PH was considered to be an appropriate candidate for **Pg29** or **Pg31**.[26] Similarly, **Pg32** and **Pg33** gave $[M - H]^-$ ions at *m/z* 651, which was 28 Da higher than **Pg21**, indicating the presence of two methoxyl groups. The formation of ions at *m/z* 475 and 329, 14 Da higher than *m/z* 461 and 315 of **Pg21**, revealed that one methoxyl group was present in the caffeoyl unit, and another one might be present in the phenylethyl moiety. Cistanoside D derived from PH was considered to be an appropriate candidate for **Pg32** and **Pg33**.[27]

Pg4 gave an $[M - H]^-$ ion at *m/z* 299.1129 ($C_{14}H_{19}O_7$), 324 Da less than **Pg21**, and had the same fragmentation pathway as that of **Pg21**, indicating the absence of caffeoyl, rhamnose and hydroxyl. Therefore, salidroside derived from FF was considered to be an appropriate candidate for **Pg4**.[28] Similarly, **Pg5** was assigned as forsythoside E.[23]

Pg15 and **Pg20** produced identical molecular ions to **Pg26**, and fragmented in the same way. They were thus assigned as calceolarioside B isomers. According to the literature, calceolarioside A derived from FF was considered to be the most suitable candidate for **Pg15** and **Pg20**.[29]

Type II (the β position was substituted). In contrast to **Pg21** (forsythoside A), suspensaside A showed a significantly different fragmentation pattern which resulted from the etherification of the C-2 position of glucose and the β position of the phenylethyl group. On one hand, similar to type I, its fragmentation was initially triggered by the loss of the caffeoyl moiety to yield an abundant ion at *m/z* 459, accompanied by the sequential loss of water to produce an ion at *m/z* 441. The MS^3 spectrum of *m/z* 459 gave a base peak at *m/z* 151, corresponding to losses of rhamnose (146 Da) and hexose (162 Da). On the other hand, because

Table 1 Identification of chemical constituents of XEQJ by LTQ-orbitrap (negative ion mode)

No.	t_R (min)	Component herb	Theoretical mass m/z	Experimental mass m/z	Error (ppm)	Formula $[M-H]^-$	(−)-ESI-MS^n data, P-ion (%)	Identification
Pg1	12.87	FF	477.1603	477.1606	0.781	$C_{20}H_{29}O_{13}$	MS^2[477]: 459(100), 163(5.9), 325(3.5), 151(2.6), 367(1.5), 307(1.4), 235(1.3) MS^3[459]: 151(100), 193(7.5), 163(6.7), 205(1.9), 325(1.1), 247(0.9)	Forsythoside D or other unknown isomers
Pg2	13.29	FF	477.1603	477.1605	0.530	$C_{20}H_{29}O_{13}$	MS^2[477]: 459(100), 163(7.5), 325(3.8), 151(2.6), 367(1.5), 307(1.4), 235(1.4) MS^3[459]: 151(100), 193(7.5), 163(6.7), 205(1.9), 145(0.9)	Forsythoside D or other unknown isomers
Pg3	16.70	FF	477.1603	477.1602	−0.099	$C_{20}H_{29}O_{13}$	MS^2[477]: 315(100), 221(9.1), 135(8.3), 179(7.9), 143(3.3), 459(3.2), 161(2.8)	New compound
Pg4	21.65	FF	299.1125	299.1129	1.072	$C_{14}H_{19}O_7$	MS^2[299]: 179(100), 119(71.7), 113(69.2), 143(58.3), 161(52.1), 101(16.7), 131(16.2)	Salidroside
Pg5	22.84	FF	461.1654	461.1651	−0.483	$C_{20}H_{29}O_{12}$	MS^2[461]: 315(100), 135(59.8), 281(56.4), 137(33.0) MS^3[315]: 135(100), 119(5.0), 179(4.3), 143(2.5)	Forsythoside E
Pg6	34.81	FF	639.1920	639.1915	−0.769	$C_{29}H_{35}O_{16}$	MS^2[639]: 621(100), 469(7.0), 459(1.6), 487(1.2) MS^3[621]: 469(100), 459(93.0), 441(45.2), 179(17.6), 487(15.7)	(*R*)-Suspensaside
Pg7	36.70	FF	639.1920	639.1912	−1.160	$C_{29}H_{35}O_{16}$	MS^2[639]: 621(100), 529(7.3), 469(1.8), 487(1.6), 459(1.0), 441(0.7) MS^3[621]: 469(100), 459(63.8), 441(49.0), 179(17.9)	(*S*)-Suspensaside
Pg8	39.92	RRP	785.2499	785.2494	−0.611	$C_{35}H_{45}O_{20}$	MS^2[785]: 623(100), 605(1.1), 459(0.3), 639(0.3) MS^3[623]: 461(100), 477(75.9), 459(21.2), 315(11.7), 297(2.6), 443(1.6), 605(1.4), 221(0.8)	Echinacoside
Pg9	40.93	FF	639.1920	639.1914	−0.956	$C_{29}H_{35}O_{16}$	MS^2[639.19]: 621(100), 529(12.8), 477(12.6), 487(4.2) MS^3[621]: 469(100), 459(93.0), 441(45.2), 487(15.7)	β-Hydroxyacteoside
Pg10	43.27	FF	639.1920	639.19196	−0.002	$C_{29}H_{35}O_{16}$	MS^2[639]: 477(100), 459(11.1), 315(2.8), 461(1.2), 503(1.1) MS^3[477]: 315(100), 221(11.2), 135(8.9), 143(5.7), 179(5.2), 161(3.2)	New compound
Pg11	45.54	FF	609.1814	609.1810	−0.700	$C_{28}H_{33}O_{15}$	MS^2[609]: 447(100), 429(13.1), 315(4.0), 477(3.5), 179(2.5), 473(2.1) MS^3[447]: 315(100), 135(19.5), 149(3.0), 191(2.7), 131(2.6)	Calceolarioside C or other unknown isomers
Pg12	45.90	RRP	799.2655	799.2648	−0.863	$C_{36}H_{47}O_{20}$	MS^2[799]: 623(100), 605(10.0), 461(1.6), 637(1.6), 477(0.7), 459(0.6), 653(0.3), 443(0.3) MS^3[623]: 461(100), 477(74.7), 459(20.1), 315(11.6), 297(2.3), 605(1.9), 443(1.7)	Jionoside A
Pg13	47.68	FF	623.1970	623.1959	−1.904	$C_{29}H_{35}O_{15}$	MS^2[623]: 461(100), 443(15.1), 487(3.5), 477(3.3), 178(1.9) MS^3[461]: 315(100), 135(56.8), 205(28.3), 163(18.0), 145(5.1), 143(4.5)	Forsythoside H
Pg14	48.08	FF	609.1814	609.1815	0.203	$C_{28}H_{33}O_{15}$	MS^2[609]: 447(100), 429(6.38), 477(5.61), 315(3.21), 179(1.44), 473(1.05) MS^3[447]: 315(100), 135(29.59), 149(3.53), 131(2.79), 191(1.99)	Calceolarioside C or other unknown isomers
Pg15	48.18	FF	477.1391	477.1398	1.325	$C_{23}H_{25}O_{11}$	MS^2[477]: 161(100), 315(17.5), 179(11.7), 203(4.6), 135(1.9), 323(1.3), 341(1.0)	Calceolarioside A or other unknown isomers
Pg16	49.39	FF	609.1814	609.1812	−0.306	$C_{28}H_{33}O_{15}$	MS^2[609]: 447(100), 429(7.8), 315(4.1), 477(2.8), 179(1.7), 473(1.5) MS^3[447]: 315(100), 135(21.8), 149(5.4), 191(4.0), 131(2.4)	Calceolarioside C or other unknown isomers
Pg17[a]	49.50	FF	755.2393	755.2387	−0.788	$C_{34}H_{43}O_{19}$	MS^2[755]: 593(100), 461(1.6), 623(1.6), 575(1.5) MS^3[593]: 447(100), 461(87.2), 429(21.4), 315(11.6), 297(2.3), 443(1.8)	Forsythoside B
Pg18	50.21	FF	755.2393	755.2389	−0.550	$C_{34}H_{43}O_{19}$	MS^2[755]: 593(100), 461(1.6), 623(1.6), 575(1.5) MS^3[593]: 447(100), 461(87.2), 429(21.4), 315(11.6), 297(2.3), 443(1.8)	Other unknown isomers of forsythoside B
Pg19	51.15	FF	623.1970	623.1953	−2.883	$C_{29}H_{35}O_{15}$	MS^2[623]: 461(100), 443(8.7), 487(2.3), 203(1.6), 477(1.5), 179(1.5), 315(1.1), 205(0.3) MS^3[461]: 315(100), 135(55.2), 205(37.3), 163(16.6), 143(7.8), 145(5.5), 134(3.0), 162(1.3)	Forsythoside I

Table 1 (*Contd.*)

No.	t_R (min)	Component herb	Theoretical mass *m/z*	Experimental mass *m/z*	Error (ppm)	Formula $[M-H]^-$	(−)-ESI-MS^n data, P-ion (%)	Identification
Pg20	51.74	FF	477.1391	477.1390	−0.268	$C_{23}H_{25}O_{11}$	MS^2[477]: 161(100), 459(22.7), 179(22.1), 315(19.2), 271(13.2), 271(4.4), 433(4.4)	Calceolarioside A or other unknown isomers
Pg21[a]	51.78	FF	623.1970	623.1957	−2.097	$C_{29}H_{35}O_{15}$	MS^2[623]: 461(100), 443(8.7), 487(2.3), 477(1.5) MS^3[461]: 315(100), 135(62.9), 205(34.6), 163(21.3)	Forsythoside A
Pg22[a]	53.68	FF, RRP, PH	623.1970	623.1963	−1.214	$C_{29}H_{35}O_{15}$	MS^2[623]: 461(100), 443(3.53), 315(1.7), 477(1.6) MS^3[461]: 315(100), 135(52.9), 297(14.9), 161(8.5), 143(3.6), 163(1.4)	Acteoside
Pg23	54.05	FF	769.2550	769.2538	−1.528	$C_{35}H_{45}O_{19}$	MS^2[769]: 607(100), 461(2.7), 589(2.2), 623(1.6), 750(1.2), 725(1.1), 751(1.0), 443(0.6)	Forsythoside G
Pg24	55.20	RRP	813.2812	813.2802	−1.180	$C_{37}H_{49}O_{20}$	MS^2[813]: 637(100), 619(25.6), 473(4.4), 491(4.3), 475(2.3), 475(2.2), 667(1.4), 651(1.3) MS^3[637]: 491(100), 473(44.1), 475(39.6), 457(3.0), 329(2.6), 619(1.9)	Jionoside B
Pg25	54.24	FF	621.1814	621.1808	−0.977	$C_{29}H_{33}O_{15}$	MS^2[621]: 469(100), 459(65.7), 441(51.4), 202(30.6), 178(21.5), 487(18.4), 233(14.8), 205(6.2), 427(5.6), 397(3.2) MS^3[469]: 179(100), 161(89.7), 233(68.6), 203(31.1), 245(19.3), 367(14.9), 451(14.4), 409(7.4), 189(8.0)	Suspensaside A or other unknown isomers
Pg26[a]	54.69	FF	477.1391	477.1397	1.073	$C_{23}H_{25}O_{11}$	MS^2[477]: 161(100), 315(21.5), 281(2.7), 251(1.9), 179(1.8), 221(1.1), 341(0.7) MS^3[161]: 133(100), 161(5.9), 117(0.6), 105(0.4)	Calceolarioside B
Pg27	56.95	FF	621.1814	621.1810	−0.590	$C_{29}H_{33}O_{15}$	MS^2[621]: 469(100), 459(89.0), 487(59.4), 203(41.9), 441(37.4), 427(23.2), 179(20.7), 397(6.7), 367(4.7) MS^3[469]: 179(100), 161(81.6), 233(28.3), 135(20.6), 367(19.9), 203(18.7), 451(13.9), 409(12.5), 263(11.6)	Suspensaside A or other unknown isomers
Pg28[a]	57.83	RRP, PH	623.197	623.1962	−1.407	$C_{29}H_{35}O_{15}$	MS^2[623]: 461(100), 477(1.5), 443(0.8), 179(0.4) MS^3[461]: 315(100), 135(49.6), 297(16.4), 169(13.5), 143(3.6), 134(3.4)	Isoacteoside
Pg29	62.69	PH	637.2127	637.2125	−0.371	$C_{30}H_{37}O_{15}$	MS^2[637]: 461(100), 491(8.6), 443(6.7), 475(5.2), 593(1.7), 329(1.3), 315(1.3)	Leucosceptoside A or other unknown isomers
Pg30	67.60	FF	621.1814	621.1810	−0.687	$C_{29}H_{33}O_{15}$	MS^2[621]: 459(100), 251(44.2), 323(34.5), 469(32.3), 487(27.7), 179(22.8), 305(18.3) MS^3[459]: 151(100), 161(41.9), 205(20.3), 247(15.7), 313(13.1), 143(9.3), 277(8.3), 369(7.6), 307(7.4)	Suspensaside A or other unknown isomers
Pg31	68.43	PH	637.2127	637.2121	−1.031	$C_{30}H_{37}O_{15}$	MS^2[637]: 461(100), 491(10.8), 475(5.12), 538(4.0), 265(1.8), 315(1.6), 443(1.6) MS^3[461]: 315(100), 135(49.9), 161(10.5), 297(9.4), 143(4.7), 307(1.1), 179(0.8)	Leucosceptoside A or other unknown isomers
Pg32	74.55	PH	651.2283	651.2279	−0.671	$C_{31}H_{39}O_{15}$	MS^2[651]: 475(100), 505(35.4), 457(22.6), 193(18.2), 265(9.9), 329(7.8), 487(5.8)	Cistanoside D or other unknown isomers
Pg33	79.35	PH	651.2283	651.2283	−0.210	$C_{31}H_{39}O_{15}$	MS^2[651]: 475(100), 505(79.2), 193(28.9), 265(19.3), 487(13.9), 457(12.5), 337(5.6)	Cistanoside D or other unknown isomers
Pa1	3.06	FLJ	191.0550	191.0556	3.221	$C_7H_{11}O_6$	MS^2[191]: 127(100), 173(69.6), 93(50.5), 171(25.6) MS^3[127]: 85(100), 109(67.8), 99(41.9)	Quinic acid
Pa2[a]	20.44	FLJ	353.0867	353.0861	−1.667	$C_{16}H_{17}O_9$	MS^2[353]: 191(100), 179(45.4), 135(8.5), 173(2.7) MS^3[190.97]: 127(100), 173(73.3), 111(35.5), 171(30.3)	3-*O*-Caffeoylquinic acid
Pa3	26.34	FLJ	337.0918	337.0929	3.281	$C_{16}H_{17}O_8$	MS^2[337]: 163(100), 191(6.1), 119(6.1), 173(4.2), 293(1.5)	3-*p*-CoQA
Pa4[a]	28.17	FLJ	353.0867	353.0865	−0.534	$C_{16}H_{17}O_9$	MS^2[353]: 191(100), 179(3.0), 135(0.6), 161(0.3) MS^3[191]: 127(100), 85(77.0), 173(66.4)	5-*O*-Caffeoylquinic acid
Pa5[a]	29.75	FLJ	353.0867	353.0865	−1.157	$C_{16}H_{17}O_9$	MS^2[353]: 173(100), 179(52.0), 191(15.0), 135(8.2), 155(1.5) MS^3[173]: 93(100), 111(54.4), 71(23.0), 155(15.7), 109(8.1)	4-*O*-Caffeoylquinic acid
Pa6	35.68	FLJ	337.0918	337.0929	2.896	$C_{16}H_{17}O_8$	MS^2[337]: 191(100), 163(6.1) MS^3[191]: 127(100), 173(71.2), 111(35.7), 171(29.2)	5-*p*-CoQA
Pa7	36.82	FLJ	337.0918	337.0929	3.163	$C_{16}H_{17}O_8$	MS^2[337]: 173(100), 163(8.2), 191(5.1), 137(0.9) MS^3[173]: 93(100), 111(49.4), 155(9.4), 137(8.2)	4-*p*-CoQA

Table 1 (*Contd.*)

No.	t_R (min)	Component herb	Theoretical mass *m/z*	Experimental mass *m/z*	Error (ppm)	Formula $[M-H]^-$	(−)-ESI-MS^n data, P-ion (%)	Identification
Pa8	39.62	FLJ	367.1024	367.1027	0.821	$C_{17}H_{19}O_9$	MS^2[367]: 191(100), 173(15.0), 193(6.8) MS^3[191]: 127(100), 173(75.7), 93(59.0), 171(29.2)	5-Feruloylquinic acid
Pa9[a]	58.16	FLJ	515.1184	515.1182	−0.335	$C_{25}H_{23}O_{12}$	MS^2[515]: 353(100), 335(12.7), 179(9.3), 191(5.0) MS^3[353]: 173(100), 179(70.7), 191(48.0), 135(11.2), 155(1.6)	3,4-*O*-Dicaffeoylquinic acid
Pa10[a]	60.26	FLJ	515.1184	515.1187	0.597	$C_{25}H_{23}O_{12}$	MS^2[515]: 353(100), 191(1.8), 179(1.5), 335(1.1) MS^3[353]: 191(100), 179(45.7), 135(8.4), 173(6.3), 161(0.8)	3,5-*O*-Dicaffeoylquinic acid
Pa11[a]	65.05	FLJ	515.1184	515.1179	−0.937	$C_{25}H_{23}O_{12}$	MS^2[515]: 353(100), 173(5.8), 255(5.4), 317(4.4) MS^3[353]: 173(100), 179(60.4), 191(26.6), 135(9.1), 155(1.5)	4,5-*O*-Dicaffeoylquinic acid
Pa12	69.42	FLJ	529.1341	529.1342	0.316	$C_{26}H_{25}O_{12}$	MS^2[529]: 367(100), 173(20.6), 335(17.2), 193(3.6), 353(3.3), 179(2.1)	Methylated dicaffeoylquinic acid
Pa13	76.47	FLJ	529.1341	529.1341	0.203	$C_{26}H_{25}O_{12}$	MS^2[529]: 353(100), 367(32.5), 203(7.7), 173(6.0), 191(3.0), 179(2.9), 349(1.7), 193(1.0)	Methylated dicaffeoylquinic acid
F1[a]	50.47	FLJ, FF	609.1450	609.1455	0.819	$C_{27}H_{29}O_{16}$	MS^2[609]: 301(100), 300(35.0), 343(7.7) MS^3[301]: 179(100), 151(84.7), 273(15.2), 257(15.2), 199(7.7), 229(7.0), 283(5.5), 255(5.1), 107(4.9)	Rutin
F2[a]	52.99	FLJ, FF, PH	463.0871	463.0869	−0.415	$C_{21}H_{19}O_{12}$	MS^2[463]: 301(100), 300(30.3), 343(2.6), 271(1.6) MS^3[301]: 179(100), 151(74.4), 273(14.8), 257(12.5), 193(7.0), 283(5.9), 121(1.8)	Isoquercitrin
F3[a]	53.11	FLJ, FF	447.0922	447.0928	1.436	$C_{21}H_{19}O_{11}$	MS^2[447]: 285(100), 327(2.0), 403(1.1), 359(0.7) MS^3[285]: 241(100), 199(99.5), 217(77.8), 243(70.9), 151(40.4), 133(16.0), 107(9.9)	Luteoloside
F4[a]	53.71	FLJ	593.1501	593.1501	−0.011	$C_{27}H_{29}O_{15}$	MS^2[593]: 285(100), 284(24.8) MS^3[285]: 241(100), 199(97.8), 175(84.8), 243(69.2), 217(66.6), 151(41.4), 267(25.9), 257(23.1), 133(8.4)	Lonicerin
F5[a]	57.43	FLJ	593.1501	593.1506	0.798	$C_{27}H_{29}O_{15}$	MS^2[593]: 285(100), 447(10.2), 229(3.4), 257(3.3), 327(2.4), 267(1.8), 241(0.9)	Kaempferol 3-*O*-rutinoside
F6	61.44	FLJ	477.1028	477.1036	1.797	$C_{22}H_{21}O_{12}$	MS^2[477]: 314(100), 315(34.5), 271(5.3), 273(3.6), 300(3.1), 299(5.8), 151(3.8), 179(1.5)	Isorhamnetin-*O*-hexoside
F7[a]	61.51	PH	431.0972	431.0981	1.802	$C_{21}H_{19}O_{10}$	MS^2[431]: 269(100), 387(5.1), 311(3.1) MS^3[269]: 225(100), 268(84.4), 197(44.7), 227(40.5), 224(40.3), 183(40.0), 149(37.5), 169(35.1)	Apigetrin
F8	62.77	FLJ	607.1657	607.1660	0.335	$C_{28}H_{31}O_{15}$	MS^2[607]: 299(100), 284(39.3), 443(5.8), 285(4.2), 487(3.0)	Chrysoeriol-7-*O*-neohesperidoside
F9	63.05	FLJ	637.1763	637.1765	0.218	$C_{29}H_{33}O_{16}$	MS^2[637]: 461(100), 491(6.3), 443(6.2), 329(5.8), 475(4.4), 193(1.8)	Tricin-7-*O*-neohesperidoside
F10[a]	63.51	FLJ	461.1078	461.1089	2.217	$C_{22}H_{21}O_{11}$	MS^2[461]: 299(100), 446(73.5), 298(12.3), 284(10.3) MS^3[299]: 284(100), 297(0.7), 269(0.6), 285(0.2), 255(0.2), 271(0.2), 219(0.1), 187(0.1), 199(0.1)	Diosmetin-7-*O*-glucoside
F11[a]	63.53	FLJ	491.1184	491.1190	1.196	$C_{23}H_{23}O_{12}$	MS^2[491]: 476(100), 329(57.3), 328(11.9), 314(11.1) MS^3[476]: 343(100), 314(95.5), 461(53.72), 313(34.8), 315(24.9), 327(13.0)	Tricin-7-*O*-glucoside
L1	45.78	FF	535.1810	535.1810	0.051	$C_{26}H_{31}O_{12}$	MS^2[535]: 373(100), 313(3.3), 343(2.6), 371(0.4), 267(0.4), 517(0.8) MS^3[373]: 313(100), 343(55.8), 325(7.2), 358(3.3), 355(0.8), 310(0.4), 181(0.1)	(+)-1-Hydroxylpinoresinol-*O*-glucoside
L2	55.76	FF	519.1861	519.1860	−0.093	$C_{26}H_{31}O_{11}$	MS^2[519]: 357(100), 389(0.6), 399(0.5) MS^3[357]: 151(100), 136(38.1), 311(13.0), 342(10.3), 327(3.3), 175(2.9)	(+)-Pinoresinol-*O*-glucoside
L3	59.29	FF	519.1861	519.1872	2.122	$C_{26}H_{31}O_{11}$	MS^2[565]: 357(100), 519(25.1) MS^3[357]: 151(100), 136(38.1), 311(13.0), 342(10.3), 327(3.3), 175(2.9)	(+)-Epipinoresinol-4″-*O*-glucoside
L4	60.64	FF	519.1861	519.1874	2.488	$C_{26}H_{31}O_{11}$	MS^2[565]: 357(100), 519(35.5), 521(2.2), 547(1.8) MS^3[357]: 151(100), 136(38.1), 311(13.0), 342(10.3), 327(3.3), 175(2.9)	(+)-Epipinoresinol-4′-*O*-glucoside
L5	63.97	FF	373.1282	373.1285	0.725	$C_{20}H_{21}O_7$	MS^2[373]: 313(100), 343(55.2), 325(4.7), 358(2.9), 355(0.4), 327(0.3) MS^3[313]: 298(100), 136(6.2), 188(4.6), 189(3.5), 108(2.1), 174(1.2)	(+)-1-Hydroxylpinoresinol

Table 1 (*Contd.*)

No.	t_R (min)	Component herb	Theoretical mass *m/z*	Experimental mass *m/z*	Error (ppm)	Formula $[M-H]^-$	(−)-ESI-MS^n data, P-ion (%)	Identification
L6	65.85	FF	519.1861	519.1864	0.601	$C_{26}H_{31}O_{11}$	MS^2[519]: 357(100), 353(0.3), 399(0.3), 501(0.1), 355(0.1), 313(0.1) MS^3[357]: 313(100), 342(52.3), 209(45.4), 298(42.2), 147(32.3), 281(17.0), 162(7.5)	Matairesinoside
L7	70.18	FF	533.2017	533.2032	2.761	$C_{27}H_{33}O_{11}$	MS^2[579]: 371(100), 263(99.5), 296(29.2), 533(20.7), 248(18.5), 233(17.2)	Pinoresinol monomethyl ether *O*-glucoside
L8	74.27	FF	371.1489	371.1488	−0.390	$C_{21}H_{23}O_6$	MS^2[371]: 356(100), 326(3.1), 341(1.0), 327(0.9), 151(0.5) MS^3[356]: 121(100), 135(57.0), 136(30.7), 177(30.1), 122(26.4), 341(22.6), 163(20.6), 151(14.4)	Phillygenin
L9[a]	74.27	FF	533.2017	533.2030	2.385	$C_{27}H_{33}O_{11}$	MS^2[579]: 371(100), 533(29.5), 543(3.3), 207(1.5) MS^3[371]: 356(100), 326(2.0), 341(1.1), 323(0.6)	Phillyrin
I1	13.35	RRP	523.1657	523.1656	−0.299	$C_{21}H_{31}O_{15}$	MS^2[523]: 179(100), 361(36.8), 181(35.4), 343(27.3) 487(6.4), 199(5.9)	Rehmannioside A or B
I2	18.71	FLJ, FF, RRP	375.1285	375.1286	0.151	$C_{16}H_{23}O_{10}$	MS^2[375]: 213(100), 151(6.1), 315(4.2), 285(2.8) MS^3[213]: 124(100), 169(20.9), 151(8.7)	Loganin acid
I3	22.67	FLJ	373.1129	373.1127	−0.518	$C_{16}H_{21}O_{10}$	MS^2[373]: 211(100), 167(41.7), 149(15.6), 193(11.5), 123(9.9)	Secologanic acid or other unknown isomers
I4	23.70	FLJ	375.1285	375.1287	0.471	$C_{16}H_{23}O_{10}$	MS^2[375]: 213(100), 169(15.4), 151(3.6), 125(1.7) MS^3[213]: 169(100), 125(19.6), 151(12.6), 107(10.9)	8-*epi*-Loganin acid
I5	28.28	FLJ	389.1078	389.1078	−0.123	$C_{16}H_{21}O_{11}$	MS^2[389]: 345(100), 209(29.0), 121(19.5), 165(13.8) MS^3[345]: 165(100), 183(76.7), 179(47.3), 113(42.4), 119(39.3)	Secologanoside
I6	29.18	FLJ	373.1129	373.1131	0.474	$C_{16}H_{21}O_{10}$	MS^2[373]: 193(100), 149(30.8), 167(5.4), 179(2.8), 123(1.7) MS^3[193]: 149(100), 93(7.2), 121(2.5), 131(2.1), 107(1.0)	Secologanic acid or other unknown isomers
I7[a]	34.16	FLJ	357.1180	357.1190	2.776	$C_{16}H_{21}O_9$	MS^2[403]: 357(100), 195(55.4), 179(45.8), 125(17.7) MS^3[357]: 125(100), 195(46.1), 151(12.3), 167(9.7)	Sweroside
I8[a]	40.33	FLJ	403.1235	403.1239	1.097	$C_{17}H_{23}O_{11}$	MS^2[403]: 371(100), 179(21.5), 121(3. 7), 191(2.4) MS^3[371]: 121(100), 165(71.0), 209(20.7), 181(16.8), 311(7.6)	Secoxyloganin
I9	43.94	FLJ	417.1391	417.1397	1.299	$C_{18}H_{25}O_{11}$	MS^2[417]: 341(100), 237(14.8), 179(8.5), 385(5.5)	Dimethyl-secologanoside
S1[a]	80.89	FLJ	1235.6055	1235.6047	−0.634	$C_{59}H_{95}O_{27}$	MS^2[1236]: 1192(90.4), 1074(78.5), 912(23.5), 928(22.1), 735(19.7), 1056(27.1), 977(21.1), 1173(16.4)	Macranthoidin A

[a] Further confirmation in comparison with reference standards. t_R, retention time; Pg, phenylethanoid glycosides; Pa, phenolic acids; F, flavonoids; L, lignans; I, iridoid glycosides; S, saponins; FLJ: Flos Lonicerae Japonicae; FF: Forsythiae Fructus; RRP: Radix Rehmanniae Preparata; PH: Pogostemonis Herba.

of a special ether ring, neutral loss of 134 Da was easily observed and yielded a product ion at *m/z* 487, and also another ion at *m/z* 469, corresponding to the sequential loss of water. Other minor ions, such as *m/z* 427 $[487-60]^-$, and 397 $[487-90]^-$, were deduced to stem from the hexose unit.[30–32] The ion at *m/z* 469 was subjected to fragmentation to give product ions at *m/z* 409, 179, and 161, corresponding to the cleavage of hexose, [caffeic acid − H]$^-$, and [glc − H − H_2O]$^-$. According to the fragmentation information described above, **Pg25**, **Pg27**, and **Pg30** were tentatively characterized as isomers of suspensaside A, a known compound isolated from FF.[18]

The hydrogen atoms in the β position of (*R*)-suspensaside and (*S*)-suspensaside were substituted by hydroxyl groups, thus fragmentation observed in the MS^2 spectra of the $[M-H]^-$ was triggered by the initial loss of water to generate a significant ion at *m/z* 621; during the following fragmentation, ions at *m/z* 487, 469, 459, 441, 179 were observed, which was similar to suspensaside A, indicating that the ion at *m/z* 621 might have the same structure as suspensaside A.[18] The fragmentation behaviors of **Pg6**, **Pg7** and **Pg9** were consistent with that described above. Combining the elution order reported before and *C* log *P* value, **Pg6** (*C* log *P*: −2.0278), **Pg7** (*C* log *P*: −2.0278) and **Pg9** (*C* log *P*: −1.9756) were reasonably speculated as (*R*)-suspensaside, (*S*)-suspensaside and β-hydroxyacteoside, respectively.[18] The proposed fragmentation pathway of this type of phenylethanoid glycosides is shown in Fig. 4.

Pg1 and **Pg2** both gave $[M-H]^-$ ions at *m/z* 477, 162 Da less than (*R*)-suspensaside or (*S*)-suspensaside, and these

Table 2 Identification of chemical constituents of XEQJ by LTQ-orbitrap (positive ion mode)

No.	t_R (min)	Component herb	Theoretical mass *m/z*	Experimental mass *m/z*	Error (ppm)	Formula $[M+H]^+/[M+Na]^+$	(+)-ESI-MS^n data, P-ion (%)	Identification
A1	18.55	CL	531.3177	531.3156	−4.068	$C_{28}H_{43}N_4O_6$	MS^2[531]: 293(100), 222(40.9), 165(3.5), 367(1.6) MS^3[293]: 222(100), 165(1)	Kukoamine B
A2	49.49	CL	302.1389	302.1379	−2.564	$C_{17}H_{20}NO_4$	MS^2[302]: 121(100), 138(98.5), 123(1.7), 165(1.3) MS^3[121]: 93(100), 103(11.9), 91(10.9), 121(1.5)	Dihydro-*N*-caffeoyltyramine
A3	60. 33	CL	634.2759	634.2743	−2.584	$C_{34}H_{40}N_3O_9$	MS^2[634]: 504(100), 497(33.1), 339(12.1), 394(11.6), 476(7.1) MS^3[504]: 394(100), 476(77.6), 339(51.3), 231(50.4)	(1,2-*trans*)-N^3-(4-Acetamidobutyl)-1-(3,4-dihydroxyphenyl)-7-hydroxy-N^2-(4-hydroxyphenethyl)-6,8-dimethoxy-1,2-dihydronaphthalene-2,3-dicarboxamide
A4	67.25	CL	874.373	874.3707	−2.658	$C_{42}H_{52}N_9O_{12}$	MS^2[874]: 856(100), 503(10.0), 486(6.1) MS^3[856]: 468(100), 424(11.1), 422(10.2)	Lyciumin A
A5	74.29	CL	314.1387	314.1380	−2.179	$C_{18}H_{20}NO_4$	MS^2[314]: 177(100), 145(9.4), 117(0.9) MS^3[177]: 145(100), 117(0.7), 149(0.6)	*trans*-*N*-Feruloyltyramine
A6	80.89	CL	897.389	897.3862	−3.063	$C_{44}H_{53}N_{10}O_{11}$	MS^2[897]: 879(85.2), 503(9.8) MS^3[879.40]: 468.23(100), 671.30(99.8), 424(24.6), 852(21.7), 422(10.6)	Lyciumin B
A7	80.94	CL	641.2494	641.2473	−3.286	$C_{36}H_{37}N_2O_9$	MS^2[641]: 504(100), 476(48.4), 339(13.2), 394(11.6), 231(4.4) MS^3[504]: 394(100), 476(90.0), 231(55.9), 339(53.5)	7-Hydroxy-1-(3,4-dihydroxy)-N^2,N^3-bis(4-hydroxyphenethyl)-6,8-dimethoxy-1,2-dihydronaphthalene-2,3-dicarboxamide
A8	81.01	CL	643.265	643.2634	−2.452	$C_{36}H_{39}N_2O_9$	MS^2[643]: 506(100), 343(43.1), 505(32.5), 325(16.7), 625(15.1), 293(13.0) MS^3[506]: 293(100), 325(79.0), 247(17.6), 369(14.2), 310(13.0), 341(12.1)	(*E*)-2-(4,5-Dihydroxy-2-{3-[(4-hydroxyphenethyl)amino]-3-oxopropyl}phenyl)-3-(4-hydroxy-3,5-dimethoxyphenyl)-*N*-(4-hydroxyphenethyl)acrylamide
A9	81.23	CL	964.4199	964.4180	−1.985	$C_{49}H_{58}N_9O_{12}$	MS^2[964]: 946(100), 576(10.0), 756(7.1), 558(4.6) MS^3[946]: 558(100), 514(18.1), 512(9.6)	Lyciumin C
A10[a]	84.15	IN	263.0815	263.0811	−1.726	$C_{16}H_{11}N_2O_2$	MS^2[263]: 219(100), 235(30.9), 245(24.8), 217(9.0) MS^3[219]: 219(100), 201(3.5), 192(3.4), 190(2.7)	Indirubin
S2	83.10	CARR	543.2565	543.2551	−2.547	$C_{28}H_{40}O_9Na$	MS^2[543]: 497(100), 525(12.7), 515(7.2), 524(6.1) MS^3[497]: 479(100), 480(40.9), 452(37.3), 302(30.7)	Glaucogenin C-*O*-β-D-thevetopyranoside

Table 2 (*Contd.*)

No.	t_R (min)	Component herb	Theoretical mass *m/z*	Experimental mass *m/z*	Error (ppm)	Formula $[M+H]^+/[M+Na]^+$	(+)-ESI-MS^n data, P-ion (%)	Identification
S3	83.71	CARR	673.3195	673.3178	−2.443	$C_{34}H_{50}O_{12}Na$	MS^2[673]: 627(100), 543(7.5), 655(5.2) MS^3[627]: 497(100), 297(57.6), 315(27.2), 353(1.7)	Cynaversicoside F
S4	84.21	CARR	831.4137	831.4125	−1.518	$C_{42}H_{64}O_{15}Na$	MS^2[831]: 785(100), 687(5.1), 641(3.1), 311(2.6) MS^3[785]: 641(100), 311(51.7), 497(19.1)	Cynaversicoside A
S5	84.40	CARR	687.3351	687.3328	−3.402	$C_{35}H_{52}O_{12}Na$	MS^2[687]: 641(100), 543(53.2), 669(17.2), 497(14.2) MS^3[641]: 497(100), 311(42.0), 329(14.2), 497(5.3)	Atratoglaucoside A
S6	84.88	CARR	817.3981	817.3957	−2.939	$C_{41}H_{62}O_{15}Na$	MS^2[817]: 771(100), 673.(74.0), 543.35(3.6) MS^3[771]: 627(100), 441(8.3), 297(5.6), 497(4.1), 353(0.3)	Glaucoside C

[a] Further confirmation in comparison with reference standards. t_R, retention time; A, alkaloids; S, saponins; CL: Cortex Lycii; CARR: Cynanchi Atrati Radix et Rhizoma; IN: Indigo Naturalis.

fragmentation patterns were identical to suspensaside A, indicating the absence of the caffeoyl unit compared to (*R*)-suspensaside or (*S*)-suspensaside. Thus, forsythoside D derived from FF was considered to be an appropriate candidate for **Pg1** and **Pg2**.[33]

3.2.2 Structural characterization and identification of phenolic acids. The structure of phenolic compounds consisted of esters formed between quinic acid and one to four residues of certain *trans*-cinnamic acids, commonly including caffeic, *p*-coumaric, ferulic, and sinapic. A total of 13 phenolic acids were screened from XEQJ, which were all from FLJ. Their characteristic fragmentation pathways were first characterized by the loss of one or two cinnamic acid moieties and successively by dehydration.[34] Besides, a quinic acid moiety at *m/z* 191, a dehydrated quinic acid moiety at *m/z* 173, a cinnamic acid moiety at *m/z* 179 [caffeic acid − H]$^-$, 193 [ferulic acid − H]$^-$, and 163 [coumaric acid − H]$^-$, a dehydrated caffeic acid moiety at *m/z* 161 and a decarboxylated caffeic acid moiety at *m/z* 135 were also observed in their ESI-MS experiment. Peaks **Pa2**, **Pa4**, **Pa5**, **Pa9**, **Pa10**, and **Pa11** could be unambiguously identified as 3-CQA, 5-CQA, 4-CQA, 3,4-DiCQA, 3,5-DiCQA, and 4,5-DiCQA by comparison with reference compounds. Additionally, **Pa2**, **Pa4**, and **Pa5** were a group of CQA isomers, while **Pa9**, **Pa10** and **Pa11** were a group of DiCQA isomers. We could speculate the substitution position of caffeoyl according to the kind and relative intensity of the base peak in their ESI-MS^n spectra.[35] Peaks **Pa3**, **Pa6**, and **Pa7** released the [M − H]$^-$ ions at *m/z* 377 corresponding to *p*-coumaroylquinic acid (*p*-CoQA). In their MS^2 spectra, the base peak was remarkably different. Generally, esterification at positions 3, 4, 5, or 1 of the quinic acid moiety produced base peaks at *m/z* 163, 173, and 191, respectively.[36] However, the polarity of 5-*p*-CoQA is weaker than that of 3-*p*-CoQA. Thus, **Pa3**, **Pa6** and **Pa7** were identified as 3-*p*-CoQA, 5-*p*-CoQA, and 4-*p*-CoQA, respectively. Furthermore, **Pa8**, a feruloylquinic acid (FQA) that generated an ESI-MS^2 base peak at *m/z* 191, was detected. Hence, it was tentatively characterized as 5-FQA.[36] Peak **Pa1** produced a deprotonated molecular ion at *m/z* 191 and fragment ions at *m/z* 173 [M − H − H_2O]$^-$ and 127 [M − H − H_2O − H_2O − CO]$^-$. So, it was characterized as quinic acid. Peaks **Pa12** and **Pa13** exhibited [M − H]$^-$ ions at *m/z* 529 and fragment ions at *m/z* 367, 14 Da higher than *m/z* 353 in DiCQA. Thus, they were tentatively assigned as methylated dicaffeoylquinic acid.

3.2.3 Structural characterization and identification of flavonoids. A total of 11 compounds were screened and identified as flavonoids from XEQJ, among which 10 were from FLJ, 3 from FF, and 2 from PH. 8 flavonoids were unambiguously identified as rutin (**F1**), quercetin-3-*O*-glucoside (**F2**), luteolin-7-*O*-glucoside (**F3**), lonicerin (**F4**), kaempferol 3-*O*-rutinoside (**F5**), apigetrin (**F7**), diosmetin-7-*O*-glucoside (**F10**), and tricin-7-*O*-glucoside (**F11**) by comparison of retention times and mass spectra with those of reference substances.

In ESI-MS experiments, the glycosidic bond of *O*-glycosides in flavonoids was easily cleaved in the negative ion mode to produce aglycone ions (Y_0^-) of [M − H − 162]$^-$ and [M − H − 308]$^-$ corresponding to the loss of hexose sugar and rutinose unit. Sometimes, [Y_0^- − H]$^-$ occurred in the MS spectrum, especially flavonol glycosides. Dehydration, successive loss of

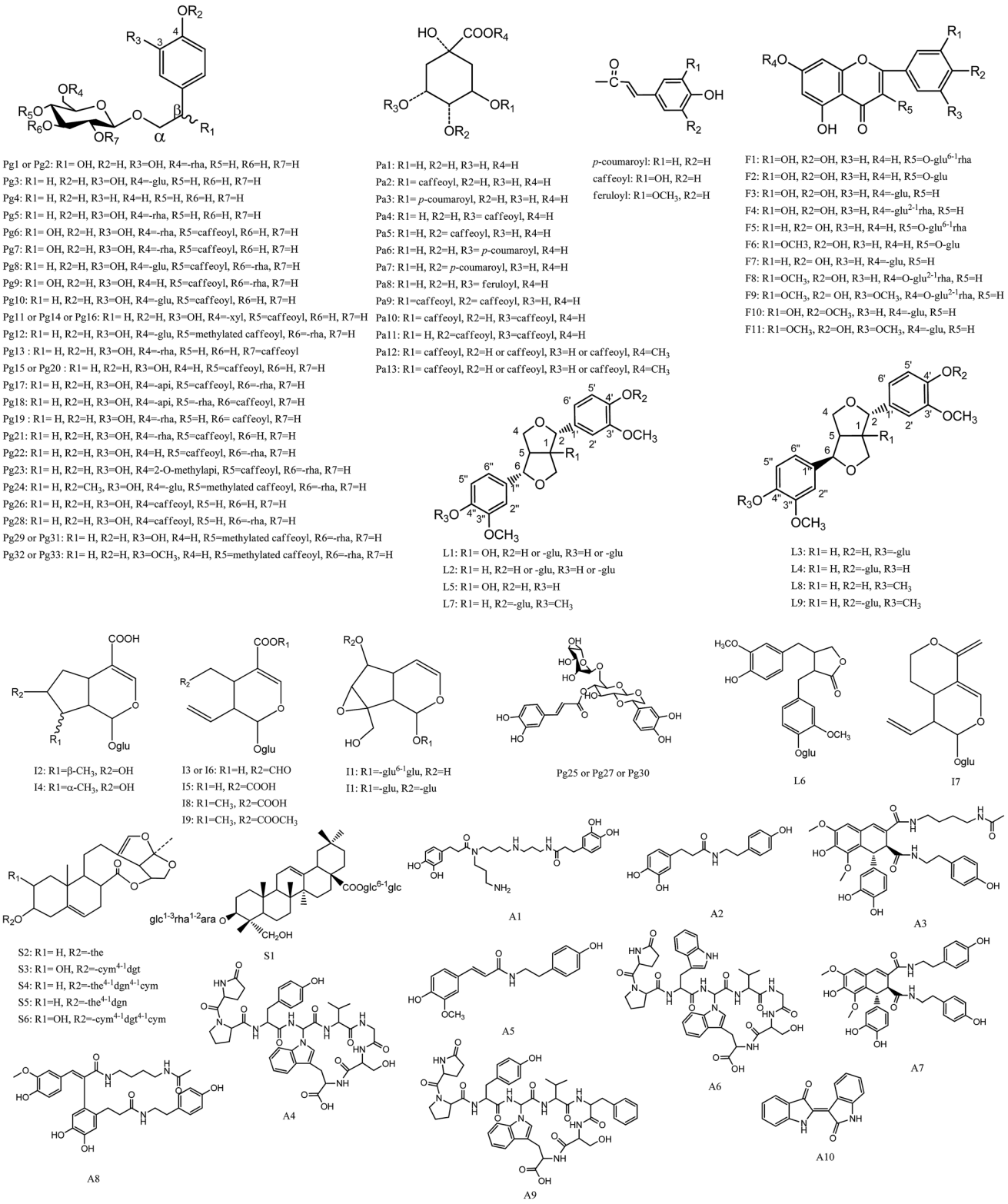

Fig. 2 Chemical structures of compounds identified in XEQJ. glu, glucose; rha, rhamnose; xyl, xylose; api, apiose; the, thevetose; cym, cymarose; dgt, digitoxose; dgn, diginose.

CO or loss of CO_2 due to the presence of phenolic hydroxyl groups and a ketone group, Retro–Diels–Alder (RDA) fragmentation, C ring fragmentation and loss of CHO· were the most possible fragmentation pathways for flavonoids.[37–39]

Here we take **F6** as an example to illustrate the fragmentation pathways of flavonoids lacking reference standards. F6 produced a high intensity $[M - H]^-$ ion at *m/z* 477.1036 ($C_{22}H_{21}O_{12}$) and Y_0^- ion at *m/z* 315 by the loss of 162 Da from

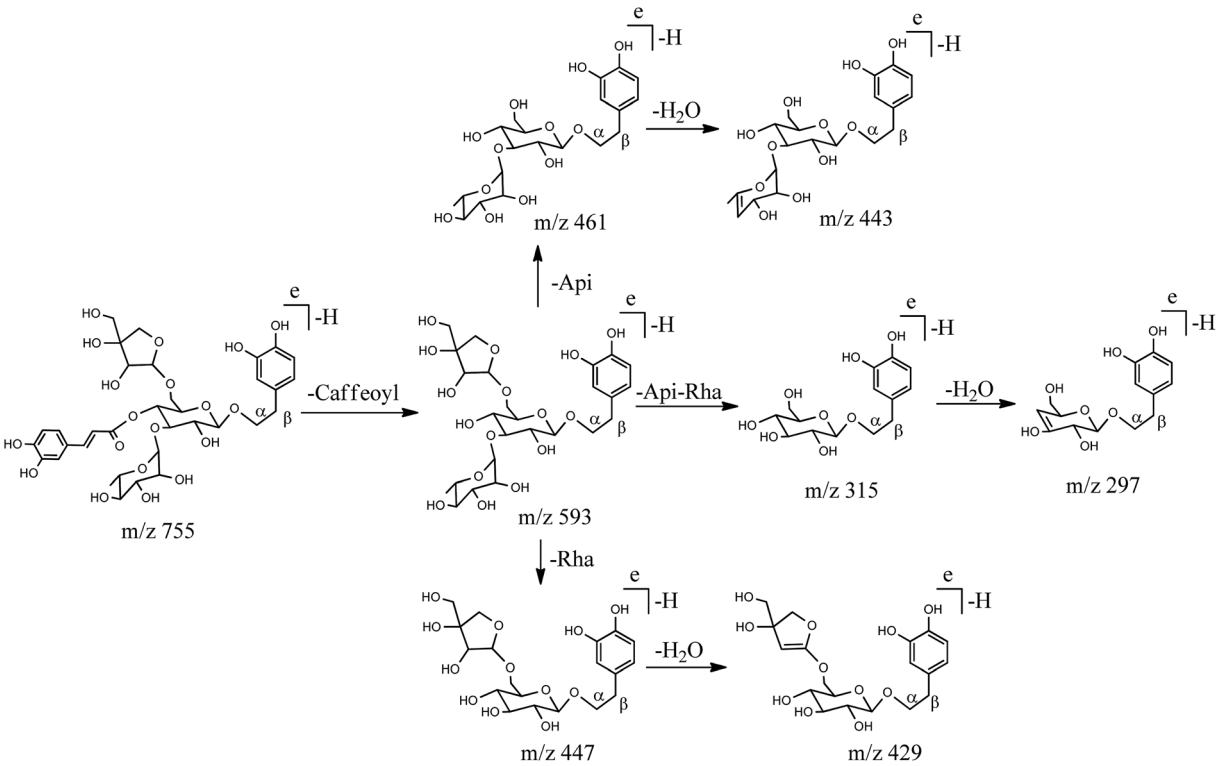

Fig. 3 The proposed fragmentation pathway of forsythoside B.

the $[M - H]^-$ ion. Further cleavage of *m/z* 315 produced other characteristic fragment ions, such as $[Y_0 - CH_3]^-$, $[Y_0 - H]^-$, $[Y_0 - H - CH_3]^-$, $[Y_0 - H - CH_3 - CO]^-$, and $^{1,3}A^-$ at *m/z* 300, 314, 299, 271, and 151, respectively. So the aglycone of **F6** was plausibly assigned as isorhamnetin. Thus, **F6** was tentatively identified as isorhamnetin-*O*-hexoside. Similarly, **F8**, a disaccharide conjugate of chrysoeriol, was tentatively identified as chrysoeriol-7-*O*-neohesperidoside and **F9**, a disaccharide conjugate of tricin, was tentatively identified as tricin-7-*O*-neohesperidoside; these compounds were previously isolated from FLJ.[40]

3.2.4 Structural characterization and identification of alkaloids. A total of 10 compounds were characterized as alkaloids, 9 of which were from CL and 1 from IN.

A10 was certainly assigned as indirubin by comparison of the retention time and mass spectra with those of the reference compound. The remaining 9 compounds, from CL, could be sorted into four types based on their different skeletons.[41]

Type I cinnamic acid amides. **A1**, **A2**, and **A5** were tentatively identified as kukoamine B, dihydro-*N*-caffeoyltyramine and *trans*-*N*-feruloyltyramine by comparison with the fragmentation ions reported in the literature.[41] **A5** gave an $[M + H]^+$ ion at *m/z* 314.1380 ($C_{18}H_{20}NO_4$). The CID of $[M + H]^+$ preferentially led to the cleavage of the amide bond to eliminate the tyramine moiety (137 Da) and produced a base ion at *m/z* 177, which could be ascribed to the feruloyl group. Further fragmentation was due to the consecutive loss of CH_3OH and CO corresponding to *m/z* 145 and 117, respectively. Compared to structure **A5**, the double bond in the caffeoyl moiety was reduced in **A2**, which resulted in a quite different fragmentation behavior in the MS^n experiment. Two predominant ions at *m/z* 138 and 121 were observed in the MS^2 spectrum. It was speculated that after the cleavage of the amide bond, electrons were transferred and eliminated of dihydrocaffeoyltyramine (164 Da) from molecular ion to generate the tyramine ion (*m/z* 138), which subsequently lost NH_3 to produce the ion of *m/z* 121. **A1** was tentatively identified as kukoamine B from its MS^n data shown in Table 1.

Type II lignanamides. Lignanamides **A3** and **A7** contained a dihydrogen naphthalene skeleton, which affected the fragmentation pattern considerably. For **A7**, it gave the $[M + H -$ tyramide$]^+$ ion at *m/z* 504 and other three characteristic ions at *m/z* 231, 394, 339. In pathway I, elimination of the 3,4-dihydroxy-*N*-(4-hydroxyphenethyl) benzamide (273 Da) moiety from $[M + H -$ tyramide$]^+$ yielded a diagnostic ion of *m/z* 231. In pathway II, characteristic ions at *m/z* 394 were formed by the neutral loss of a pyrocatechol unit (110 Da) from $[M + H -$ tyramide$]^+$. In pathway III, the other tyramide was lost from the ion of *m/z* 476 $[M + H -$ tyramide $- CO]^+$ to generate a stable ion of *m/z* 339. The fragmentation behavior observed above was consistent with previous reports. Thus, **A7** was tentatively assigned as 7-hydroxy-1-(3,4-dihydroxy)-N^2,N^3-bis(4-hydroxyphenethyl)-6,8-dimethoxy-1,2-dihydronaphthalene-2,3-dicarboxamide. Similarly, **A3** was tentatively assigned as (1,2-*trans*)-N^3-(4-acetamidobutyl)-1-(3,4-dihydroxyphenyl)-7-hydroxy-N^2-(4-hydroxyphenethyl)-6,8-dimethoxy-1,2-dihydro-naphthalene-2,3-dicarboxamide.[41]

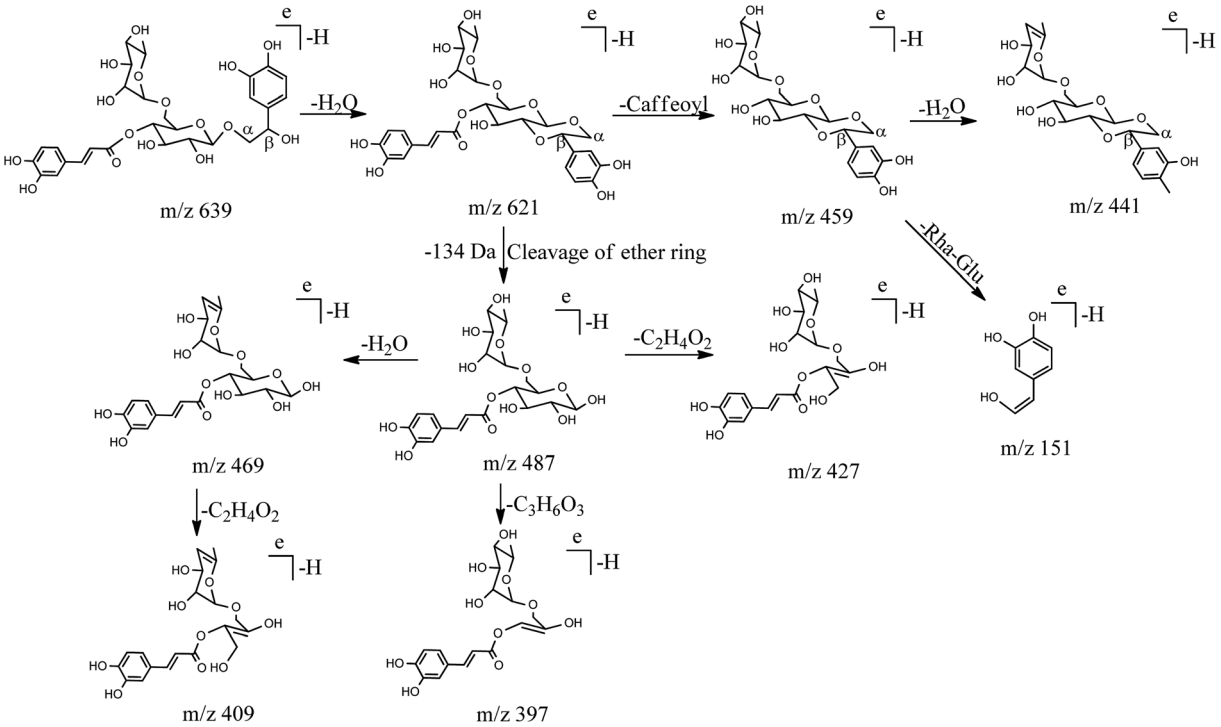

Fig. 4 The proposed fragmentation pathway of suspensaside.

Type III neolignanamides. The basic skeleton of **A8** contains a special bond between the two cinnamoyltyramine derivatives. Accordingly, its main specific fragmentation consisted of the continuous loss of two tyramide moieties, which produced the ions at *m*/*z* 506 and 369. Elimination of CO and addition of 2H yielded *m*/*z* 343 from the ion at *m*/*z* 369. Subsequent consecutive loss of H_2O and MeOH from the ion at *m*/*z* 343 produced two other ions at *m*/*z* 325 and 293. Hence, this compound was assigned as (*E*)-2-(4,5-dihydroxy-2-{3-[(4-hydroxyphenethyl) amino]-3-oxopropyl}phenyl)-3-(4-hydroxy-3,5-dimethoxyphenyl)-*N*-(4-hydroxyphenethyl) acrylamide, which had been isolated from CL.[41]

Type IV cyclic peptides. The fragmentation of cyclic peptides (compounds **A4**, **A6**, **A9**) mainly occurred in the side chain. CID of **A4** yielded a molecular ion at *m*/*z* 874.3707 ($C_{42}H_{52}N_9O_{12}$) and a dehydrated ion at *m*/*z* 856, which subsequently lost an amino acid fragment pyroGlu-Pro-Tyr (388 Da) to form the ion at *m*/*z* 468. Further fragmentation of *m*/*z* 468 was also observed. Continuous loss of HCOOH or CO_2 produced ions at *m*/*z* 422 and 424 from *m*/*z* 468. In addition, the peak at *m*/*z* 486 originated from *m*/*z* 874 by loss of the side chain (388 Da), while the peak at *m*/*z* 503 was formed by the cleavage of the amide bond to eliminate a molecular ion (371 Da) from $[M + H]^+$ ion at *m*/*z* 874. **A6** and **A9** had identical fragmentation pathways. According to the literature, **A4**, **A6** and **A9** were tentatively characterized as lyciumin A, lyciumin B and lyciumin C.[42]

3.2.5 Structural characterization and identification of lignans. A total of 9 lignans were screened from XEQJ. All of them were from FF. **L9** was unambiguously identified as phillyrin by comparison with the reference compound.

The lignans could be classified into two types according to their structural skeleton: the furofuran type (I) and the 2,3-dibenzyl butyrolactone type (II).[18]

Type I. (+)-1-Hydroxylpinoresinol underwent the characteristic cleavage of the tetrahydrofuran ring to produce the ion at *m*/*z* 343, followed by the cleavage of another tetrahydrofuran ring to yield *m*/*z* 313. The MS^n of *m*/*z* 313 showed an abundant ion at *m*/*z* 298, owing to the loss of CH_3 and another minor ion at *m*/*z* 188, owing to the loss of 110 Da from *m*/*z* 298. Successive losses of 30 Da and 110 Da were characteristics of this type of compounds.[43] **L5** generated an $[M - H]^-$ ion at *m*/*z* 373.1285 ($C_{20}H_{21}O_7$) and **L1** yielded an $[M - H]^-$ ion at *m*/*z* 535.1810 ($C_{26}H_{31}O_{12}$), 162 Da higher than **L5**; this fragmentation information was in accordance with these characteristics. Hence, **L5** and **L1** were tentatively characterized as (+)-1-hydroxylpinoresinol and (+)-1-hydroxylpinoresinol-*O*-glucoside, respectively.

As reported in the literature,[44] (+)-pinoresinol and (+)-epipinoresinol had some differences with (+)-1-hydroxylpinoresinol in the fragmentation pattern, they usually generated an $[M - H - 15]^-$ ion at *m*/*z* 342, an $[M - H - 30]^-$ ion at *m*/*z* 327 and $[M - H - 15–31]^-$ ion at *m*/*z* 311, and produced a prominent ion at *m*/*z* 151 as a result of cleavage of the tetrahydrofuran ring. **L2**, **L3** and **L4** exhibited $[M + COOH]^-$ ions at *m*/*z* 565 and $[M - H]^-$ ions at *m*/*z* 519, 162 Da higher than (+)-pinoresinol or (+)-epipinoresinol, both of which yielded an [aglycone $- H]^-$ ion at *m*/*z* 357 in their MS^2 spectrum. MS^n of *m*/*z* 357 showed similar fragmentation ions to (+)-pinoresinol or (+)-epipinoresinol. Combining the literature information about their elution behavior, they were speculated as (+)-pinoresinol-

O-glucoside, (+)-epipinoresinol-4″-*O*-glucoside and (+)-epipinoresinol-4′-*O*-glucoside, respectively.

L8 showed an $[M - H]^-$ ion at *m/z* 371.1488 ($C_{21}H_{23}O_6$), 14 Da higher than (+)-pinoresinol or (+)-epipinoresinol, and also exhibited a similar fragmentation pathway and produced ions at *m/z* 356, 341 and 326, indicating that one more methyl group existed in **L8** compared with (+)-pinoresinol or (+)-epipinoresinol. Therefore, **L8** was identified as phillygenin, tentatively.

L9 gave an $[M + COOH]^-$ ion at *m/z* 579.2063 ($C_{28}H_{35}O_{13}$) and $[M - H]^-$ ion at *m/z* 533, yielding similar fragmentation ions to **L8** (Table 1); thus, it was unambiguously identified as phillyrin with reference to the standard. **L7** possessed identical fragmentation ions and fragmentation pattern to **L9**. According to the literature, it was easily considered to be an isomer of phillyrin; thus, it was identified as (+)-pinoresinol monomethyl ether *O*-glucoside.[18]

Type II. Matairesinol, a compound with 2,3-dibenzyl butyrolactone in FS, produced an $[M - H]^-$ ion at *m/z* 357. The MS/MS spectrum of the ion at *m/z* 357 gave a significant product ion at *m/z* 313, which revealed a lactone ring in the structure. Successive elimination of CH_3 from the precursor ion at *m/z* 313, corresponding to *m/z* 298 and 283, further confirmed the presence of two methoxyl groups. The ion at *m/z* 161 was also observed owing to cleavage of the benzyl group.[18] Briefly, compounds of this type could be rapidly recognized by the loss of CO_2 and cleavage of the benzyl group. **L6** gave an $[M - H]^-$ ion at *m/z* 519, 162 Da higher than matairesinol, and it had identical fragmentation pathway to matairesinol; thus, it was rapidly characterized as matairesinoside.[45]

3.2.6 Structural characterization and identification of iridoid glycosides. Iridoid glycosides generally contain a glucose moiety attached to the C-1 position in the pyran ring. A total of 9 compounds were screened and identified as iridoid glycosides with their retention time and MS data shown in Table 1. Among them, 8 were from FLJ, 2 were from RRP and 1 from FF. Compounds of this category commonly eliminate a glucose unit (162 Da) in the pyran ring and subsequent losses of H_2O, CO_2 and CO. Neutral elimination of CH_3OH was also generally observed in methoxylated iridoid glycosides. These observations were consistent with previous studies.[46,47]

Peaks **I7** and **I8** were unambiguously characterized to be sweroside and secoxyloganin, respectively, by comparison with reference compounds. **I7** generated a predominant $[M + COOH]^-$ at *m/z* 403.1236 ($C_{17}H_{23}O_{17}$) and $[M - H]^-$ at *m/z* 357. An obvious fragment ion $[M - H - glc]^-$ at *m/z* 195 was characterized by the loss of the neutral glucose unit. Successive losses of CO_2 and CO from $[M - H - glc]^-$ yielded two more ions at *m/z* 151 and 167. Another minor ion at *m/z* 125 originated from RDA cleavage in the aglycone moiety.

I1 produced an $[M - H]^-$ ion at *m/z* 523.1656 ($C_{21}H_{31}O_{15}$) and also generated other ions such as $[M - H - glc]^-$, $[M - H - glc - glc]^-$, $[M - H - H_2O]^-$, $[M - H - H_2O - H_2O]^-$, $[M - H - H_2O - glc]^-$, $[M - H - H_2O - glc - glc]^-$ corresponding to *m/z* 361, 199, 505, 487, 343, and 181, respectively. According to these fragmentation ions, **I1** was tentatively identified as rehmannioside A or its other isomer present in RRP. **I2** and **I4**, two isomers, yielded identical $[M - H]^-$ ions at *m/z* 375, according to their ESI-MS data in Table 1. Loganin acid and 8-*epi*-loganin acid were suitable candidates for **I2** and **I4**.[37] **I5**, which generated an $[M - H]^-$ ion at *m/z* 389.1078 ($C_{16}H_{21}O_{11}$) and other fragmentation ions at *m/z* 345, 183, 165, formed by $[M - H - CO_2]^-$, $[M - H - CO_2 - glc]^-$, and $[M - H - CO_2 - glc - H_2O]^-$, was tentatively characterized as secologanoside.[48] **I3** and **I6**, both exhibited deprotonated molecular ions at *m/z* 373, 16 Da (O) less than that of **I5**, and other fragmentation ions like $[M - H - glc]^-$ at *m/z* 211, $[M - H - glc - CO_2]^-$ at *m/z* 167, $[M - H - glc - CO_2 - H_2O]^-$ at *m/z* 149, and $[M - H - glc - CO_2 - H_2O - C_2H_2]^-$ at *m/z* 123 were observed in their MS spectrum. Thus, they were characterized as secologanic acid.[49] **I9** yielded a deprotonated molecular ion at *m/z* 417.1397 ($C_{18}H_{25}O_{11}$), 28 Da (2 CH_2) higher than that of **I5**, and also produced other characteristic ions such as $[M - H - glc - H_2O]^-$ at *m/z* 237, $[M - H - CH_3OH]^-$ at *m/z* 385, and $[M - H - CH_3OH - CO_2]^-$ at *m/z* 341. Thus, **I9** could tentatively be assigned as dimethylsecologanoside.[37]

3.2.7 Structural characterization and identification of saponins. A saponin molecule consists of an aglycone and sugar units. In this study, a total of 6 saponins were characterized, in which 1 compound, from FLJ, was a triterpenoid saponin and the other 5 compounds, from CARR, were all C_{21} steroidal saponins.

S1 was unambiguously identified as macranthoidin A by comparison with the reference standard. Under negative ion mode, **S1** yielded deprotonated molecular ions at *m/z* 1235; successive loss of glucose and rhamnose gave other ions at *m/z* 1073 $[M - H - glc]^-$, 927 $[M - H - glc - rha]^-$, and 911 $[M - H - glc - glc]^-$.

The MS^n spectra in positive ion mode of C_{21} steroidal saponins provided a wealth of structural information. This type of saponins tended to generate $[M + Na]^+$, and showed an abundant ion for the loss of HCOOH (46 Da) explained by a McLafferty rearrangement from $[M + Na]^+$.[50] Fragmentation ions formed by losses of a series of sugar residues and oligosaccharide plus sodium were also observed in their spectrum. The fragmentation pattern observed was consistent with previous publication.[50] Compounds **S2**, **S3**, **S4**, **S5** and **S6** were both C_{21} steroidal saponins, and they were tentatively assigned as glaucogenin C-*O*-β-D-thevetopyranoside, cynaversicoside F, cynaversicoside A, atratoglaucoside A and glaucoside C by comparison with the literature.[50–52] Here, we take **S6** (glaucoside C) as an example to elaborate the fragmentation pathways of C_{21} steroidal saponins. **S6** produced $[M + Na]^+$ at *m/z* 817.3957 ($C_{41}H_{62}O_{15}Na$) and gave a high intensity ion $[M + Na - HCOOH]^+$ at *m/z* 771. Ions such as *m/z* 627, 497 and 353 corresponded to the successive losses of cymarose, digitoxose and cymarose from $[M + Na - HCOOH]^+$. The other two ions at *m/z* 291 and 441 were observed owing to $[cym + dgt + Na]^+$ and $[cym + dgt + cym + Na]^+$. Besides, continuous losses of cymarose and digitoxose from $[M + Na]^+$ were also observed with the formation of ions at *m/z* 673 and 543.

All the other C_{21} steroidal saponins showed a similar fragmentation pattern to that described above for S6, and their structures were elucidated by analyzing their tandem mass spectra.[53]

4. Conclusion

Our study took the advantage of the LTQ-orbitrap mass spectrometry system and reported the identification of 91 compounds with multiple structure types including phenylethanoid glycosides, phenolic acids, flavonoids, alkaloids, lignans, iridoid glycosides and saponins. The results clearly elucidated the potential fragmentation pathway of the multi-groups of constituents in XEQJ and this method has also been shown to be an excellent tool for their systematic characterization. This research not only provides abundant information for the identification and better understanding of the chemical compounds in XEQJ, but also benefits further quality control of XEQJ. Moreover, this study sets a good example for the rapid identification of complex chemical constituents in TCM and opens perspectives for similar studies on other Chinese herbal preparations.

Abbreviations

HPLC-LTQ-Orbitrap	High performance liquid chromatography coupled with linear ion trap-orbitrap mass spectrometry
XEQJ	Xiao-er-qing-jie granules
TCM	Traditional Chinese medicine
ESI	Electrospray ionization
CID	Collision induced dissociation
FLJ	Flos Lonicerae Japonicae
FF	Forsythiae Fructus
CL	Cortex Lycii
IN	Indigo Naturalis
CARR	Cynanchi Atrati Radix et Rhizoma
RRP	Radix Rehmanniae Preparata
PH	Pogostemonis Herba
HRMS	High-resolution mass spectrometry
CE	Collision energy
TIC	Total ion chromatogram
EIC	Extracted ion chromatogram

Acknowledgements

The authors greatly appreciate the financial support from the National Basic Research and Development Program of China (no. 2013-JYBZZ-XS-062).

References

1 W. H. Xie and G. X. Pang, *Hebei Med. J.*, 2004, **08**, 670–671.
2 X. Shen, M. Hou and Y. P. Song, *Journal of Gansu College of Traditional Chinese Medicine*, 2012, **29**, 4–7.
3 Ministry of health of the People's Republic of China, *National Standard for Chinese Patent Drugs*, 1993, WS3-B-1494-93.
4 Y. Q. Feng, Q. Wang and B. Liu, *Guiding Journal of TCM*, 2007, **13**, 71–72.
5 X. Q. Su and Y. P. Huang, *China Pharm.*, 2013, **16**, 1428–1430.
6 L. H. Feng, Y. X. Xiong and F. Jiang, *Journal of Jiangxi University of Traditional Chinese Medicine*, 2005, **17**, 47.
7 S. P. He and H. L. Chen, *China Pharm.*, 2011, **20**, 21–22.
8 P. Q. Huang and Y. P. Huang, *Chinese Journal of Ethnomedicine and Ethnopharmacy*, 2012, **21**, 47–48.
9 A. H. Liu, Y. H. Lin, M. Yang, H. Guo, S. H. Guan, J. H. Sun and D. A. Guo, *J. Chromatogr. B: Anal. Technol. Biomed. Life Sci.*, 2007, **846**, 32–41.
10 M. Yang, J. H. Sun, Z. Q. Lu, G. T. Chen, S. H. Guan, X. Liu, B. H. Jiang, M. Ye and D. A. Guo, *J. Chromatogr. A*, 2009, **1216**, 2045–2062.
11 J. L. Zhou, L. W. Qi and P. Li, *J. Chromatogr. A*, 2009, **1216**, 7582–7594.
12 Y. Tu, L. H. Zhao, L. Zhu, G. J. Wang and B. R. Xiang, *J. Chromatogr. Sci.*, 2004, **42**, 177–183.
13 X. J. Yu, J. Y. Zhang, Q. Q. Liu, Z. S. Wu, S. S. Liu, H. Shi and Q. Ma, *Res. J. Chem. Environ.*, 2013, **17**, 16–27.
14 J. Y. Zhang, J. Q. Lu, X. Y. Gao, Q. Zhang, N. Li, P. F. Tu and Y. J. Qiao, *Chin. J. Nat. Med.*, 2013, **11**, 63–70.
15 J. Y. Zhang, Z. J. Wang, Q. Zhang, F. Wang, J. Q. Lu and Y. J. Qiao, *Talanta*, 2014, **124**, 111–122.
16 J. B. Peng, H. M. Jia, Y. T. Liu, H. W. Zhang, S. Dong and Z. M. Zou, *J. Pharm. Biomed. Anal.*, 2011, **55**, 984–995.
17 Y. Liang, G. J. Wang, L. Xie and L. S. Sheng, *Curr. Drug Metab.*, 2011, **12**, 329–344.
18 H. Guo, A. H. Liu, M. Ye, M. Yang and D. A. Guo, *Rapid Commun. Mass Spectrom.*, 2007, **21**, 715–729.
19 D. Ryan, K. Robards, P. Prenzler, D. Jardine, T. Herlt and M. Antolovich, *J. Chromatogr. A*, 1999, **855**, 529–537.
20 Y. H. Choi, J. Kim and K. P. Yoo, *Chromatographia*, 2003, **57**, 73–79.
21 H. Kirmizibekmez, P. Montoro, S. Piacente, P. Cosimo, A. Donmez and I. Calis, *Phytochem. Anal.*, 2005, **16**, 1–6.
22 Y. Z. Zhang, F. Xu, J. Dong, J. Liang, Y. Hashi, M. Y. Shang, D. H. Yang, X. Wang and S. Q. Cai, *J. Pharm. Biomed. Anal.*, 2012, **70**, 425–439.
23 C. Li, Y. Dai, Y. H. Duan, M. L. Liu and X. S. Yao, *Chin. J. Nat. Med.*, 2014, **12**, 697–699.
24 J. Xie, J. Deng, F. Tan and J. Sun, *J. Chromatogr. B: Anal. Technol. Biomed. Life Sci.*, 2010, **878**, 2665–2668.
25 X. N. Li, M. Y. Zhou, P. Q. Shen, J. B. Zhang, C. Chu, Z. W. Ge and J. Z. Yan, *China J. Chin. Mater. Med.*, 2011, **36**, 3125–3129.
26 I. Çaliş, M. Hosny, T. Khalifa and P. Ruedi, *Phytochemistry*, 1992, **31**, 3624–3626.
27 Y. B. Li, J. Li, P. Li and P. F. Tu, *Acta Pharmacol. Sin.*, 2005, **40**, 722–727.
28 K. Endo, K. Seya and H. Hikino, *Tetrahedron*, 1989, **45**, 3673–3682.
29 Y. J. Chen, H. G. Zhang and X. Li, *Chem. Nat. Compd.*, 2009, **45**, 330–332.
30 R. E. March, X. S. Miao and C. D. Metcalfe, *Rapid Commun. Mass Spectrom.*, 2004, **18**, 931–934.
31 M. Yang, J. H. Sun, Z. Q. Lu, G. T. Chen, S. H. Guan, X. Liu, B. H. Jiang, M. Ye and D. A. Guo, *J. Chromatogr. A*, 2009, **1216**, 2045–2062.

32 S. F. Wang, Y. M. Xu, P. H. Chen and Y. F. Zhang, *Rapid Commun. Mass Spectrom.*, 2014, **28**, 1569–1579.
33 F. N. Wang, Study on the chemical constituents of Forsythia suspense (Thunb.) vahl, Chinese Academy of Medical Science Peking Union Medical College, 2009.
34 T. Zhao, J. He, X. X. Wang, B. Z. Ma, X. X. Wang, L. Zhang, P. Li, N. Liu, J. Lu and X. L. Zhang, *J. Pharm. Biomed. Anal.*, 2014, **98**, 311–320.
35 M. N. Clifford, S. Knight and N. Kuhnert, *J. Agric. Food Chem.*, 2005, **53**, 3821–3832.
36 I. Parveen, M. D. Threadgill, B. Hauck, I. Donnison and A. Winters, *Phytochemistry*, 2011, **72**, 2376–2384.
37 L. W. Qi, C. Y. Chen and P. Li, *Rapid Commun. Mass Spectrom.*, 2009, **23**, 3227–3242.
38 J. Y. Zhang, F. Wang, H. Zhang, J. Q. Lu and Y. J. Qiao, *Phytochem. Anal.*, 2014, **25**, 405–414.
39 R. Jaiswal, H. Muller, A. Muller, M. G. E. Karar and N. Kuhnert, *Phytochemistry*, 2014, **108**, 252–263.
40 J. Chen, S. L. Li, P. Li, Y. Song, X. Y. Chai and D. Y. Ma, *J. Sep. Sci.*, 2005, **28**, 365–372.
41 J. X. Zhang, S. H. Guan, J. H. Sun, T. Liu, P. Chen, R. H. Feng, X. Chen, W. Y. Wu, M. Yang and D. A. Guo, *Anal. Bioanal. Chem.*, 2014, **407**, 581–595.
42 J. X. Zhang, S. H. Guan, M. Yang, R. H. Feng, Y. Wang, Y. B. Zhang, X. Chen, X. H. Chen, K. S. Shun and D. A. Guo, *J. Pharm. Biomed. Anal.*, 2013, **77**, 63–70.
43 J. Huang, Q. Shao, Y. H. Xiang, Z. W. Ge and X. H. Fan, *China J. Chin. Mater. Med.*, 2014, **39**, 2513–2520.
44 X. Huang, F. R. Song, Z. Q. Liu and S. Y. Liu, *Anal. Chim. Acta*, 2008, **615**, 124–135.
45 I. Boldizsar, Z. Fuzfai, F. Toth, E. Sedlak, L. Borsodi and I. Molnar-Perl, *J. Chromatogr. A*, 2010, **1217**, 1674–1682.
46 L. L. Ren, X. Y. Xue, F. F. Zhang, Y. C. Wang, Y. F. Liu, C. M. Li and X. M. Liang, *Rapid Commun. Mass Spectrom.*, 2007, **21**, 3039–3050.
47 N. E. Es-Safi, L. Kerhoas and P. H. Ducrot, *Rapid Commun. Mass Spectrom.*, 2007, **21**, 1165–1175.
48 E. H. Liu, Q. Liu, C. Chu and P. Li, *J. Sep. Sci.*, 2011, **34**, 2566–2575.
49 S. Sun, Z. S. Xie, E. H. Liu, Y. T. Yan, X. J. Xu and P. Li, *Chin. J. Nat. Med.*, 2014, **12**, 229–240.
50 Z. G. Zheng, W. D. Zhang, L. Y. Kong, M. J. Liang, H. L. Li, M. Lin, R. H. Liu and C. Zhang, *Rapid Commun. Mass Spectrom.*, 2007, **21**, 279–285.
51 M. J. Liang, Z. G. Zheng, Y. Yuan, L. Y. Kong, Y. H. Shen, R. H. Liu, C. Zhang and W. D. Zhang, *Phytochem. Anal.*, 2007, **18**, 428–435.
52 H. X. Lou, X. Li and T. R. Zhu, *Acta Pharmacol. Sin.*, 1991, **27**, 595–602.
53 X. Y. Li, H. X. Sun, Y. P. Ye, F. Y. Chen and Y. J. Pan, *Steroids*, 2006, **71**, 61–66.

